Journal of Alloys and Compounds, 190 (1993) 219–227
JALCOM 474

The lead–zirconium system: binary phases and a series of interstitial compounds of the host Zr_5Pb_3

Young-Uk Kwon and John D. Corbett*
Department of Chemistry and Ames Laboratory DOE, Iowa State University, Ames, IA 50011 (USA)

(Received July 16, 1992)

Abstract

The Pb–Zr system contains the phases $Zr_{\sim 5.8}Pb$ (Cr_3Si-type), Zr_5Pb_3 (Mn_5Si_3) and Zr_5Pb_4 (Ti_5Ga_4). Zr_5Pb_4 has a substoichiometric region above approximately 800 °C, extending to about $Zr_5Pb_{3.65}$ at 1000 °C. Reactive powder sintering in sealed Ta containers at 1000–1350 °C is the most effective route for the synthesis of pure phases of both the binaries and the interstitial derivatives Zr_5Pb_3Z. Twenty examples of the latter were obtained with Z = Al, Si, P, S, Fe, Co, Ni, Cu, Zn, Ga, Ge, As, Se, Ag, Cd, In, Sn, Sb, Te, (Pb), (second period Z were not investigated). Single crystals for Z = Al, Cd, Zn, $Pb_{0.87}$, $Pb_{0.94}$ were obtained by metal flux or vapor phase transport reactions, and the last three were quantified by X-ray crystallography. Volume trends as a function of group and period follow metal/covalent radii trends for Z fairly well.

1. Introduction

Two-phases have been reported to form in the Pb–Zr system, namely, Zr_5Pb_3 [1, 2] (hexagonal, Mn_5Si_3-type) and either Zr_5Pb [3] or Zr_3Pb [4] (cubic, Cr_3Si-type). The purities, lattice parameters and compositions have not been confirmed, especially for the second phase, and the possibility of analogues of Zr_5Sn_4 or $ZrSn_2$ [5] has not been established. Almost nothing is known regarding the phase relationships [6]. The phase Zr_5Pb_3 has recently attracted interest as a potential neutron multiplier in nuclear fusion power generation [7, 8]. Donne *et al.* [9] subsequently investigated the synthesis of Zr_5Pb_3 for this purpose. They assumed the overall phase behavior of the Zr–Pb system was like those of the partially known Zr–Sn and Zr–Ge systems. Their best Zr_5Pb_3 products were obtained by hot isostatic pressing of the elemental powders in steel containers at 870 °C and 150 MPa, but they were not able to get a very pure product, and they did not know about the very similar Zr_5Pb_4.

The related phases Zr_5Sn_3 and Zr_5Sb_3 with the same Mn_5Si_3-type structure have recently been thoroughly studied with regard to their places in the binary systems [5, 10] as well as the numerous interstitial (Z) compounds each forms with the general compositions Zr_5Sn_3Z [11] and Zr_5Sb_3Z [12]. The approximately 15 Z elements that can be so bound in each host range from late transition elements to chalcogens and span periods two to five. Both hosts are electron-rich and metallic, and the similar interstitial ranges with each imply that localized Zr–Z interactions may be a major factor in the stability of the ternary products. In this context, it was deemed worthwhile not only to determine the role of common impurities on the stability of the supposed Zr_5Pb_3 binary, including the self-interstitial that might exist as Zr_5Pb_{3+x}, $0 \leq x \leq 1$, but also to examine the effect that the larger interstitial hole in Zr_5Pb_3 might have on the range of Z possible. Rieger *et al.* [13] have reported the synthesis of such a Zr_5Pb_3Cu derivative with a plausible hexagonal unit cell.

2. Experimental section

2.1. Materials

Reactor-grade zirconium was utilized in all sample preparations. The details of its cleaning and the generation of powder from zirconium strips have been described previously [5, 10]. Electrolytic lead bar (Ames Lab., 99.9999%) was scraped free of surface oxidation, cold-rolled to 2–3 mm sheet, and cut to the appropriate size.

The other reagents were: Al (United Mineral & Chemical, high purity), Si (Ames Lab., zone refined crystal bar), P (Aldrich, 99.999%), S (Alfa, 99.999%), Cr and Mn (A. D. Mackay), Fe (Plastic Metals, 99.9%), Co (Aesar, 99.9+%), Ni (Matheson, Coleman & Bell,

*Author to whom correspondence should be addressed.

0925-8388/93/$6.00

reagent), Cu (J. T. Baker Chem., 99.99%), Zn (Fisher Scientific, 99.99%), Ga (Johnson Matthey, 99.99%), Ge (Johnson Matthey, 99.999%), As (Aldrich, 99.9999%), Se (American Smelting & Refining, 99.999%), Ag (G. Frederick Smith Chem., reagent) Cd and In (Comico Products), Sn (Baker's Analyzed, 99.99%) Sb (Allied Chemical, reagent), and Te (United Mineral & Chemical, 99.999%). Most of the reagents were used as received except that Ni was first boiled in conc. aq. HCl, Zn was distilled, and the surfaces of Cd and In were scraped clean before use. Potential compounds with Z≡B, C, N, O were not studied although most probably form.

2.2. *Syntheses*

All powdered or ground reactants were prepared and handled only in a glovebox. The new and the lead-richest phase in the system, Zr_5Pb_4, was best synthesized from stoichiometric amounts of lead lump and Zr powder in a sealed Ta tube at 800–1000 °C for 3–7 days. The best route to Zr_5Pb_3 was through sintering of powdered Zr and Zr_5Pb_4 at 1000 °C. Except for a few reactions of $Zr_{4-6}Pb$ compositions and the synthesis of chalcogen and pnictogen interstitial phases, preparative reactions for Zr_5Pb_3Z were usually through sintering of pressed pellets of Zr, Zr_5Pb_4, and ZrZ_x powders sealed in welded tantalum tubing. The Ta containers were in turn jacketed in baked and well evacuated silica tubes. Powdered Zr_5Pb_3Z samples in general appear to react with air over a few days. Volatilization of lead during arc-melting reactions is so great that even a conventional weight-loss correction may not be meaningful. A few $Zr_{\sim 5}Pb$ samples, for which lead volatilization was less severe, were prepared for energy dispersive X-ray (EDX)/scanning electron microscopy (SEM) experiments by arc-melting followed by annealing treatments of 1000 °C for 7 days.

The ZrZ_x reagents were selected for their ease of grinding. These were prepared as follows: $ZrAl_2$, $ZrCr_2$, $ZrMn_2$, $ZrFe_2$, $ZrCo_2$, $ZrNi_2$, and Zr_3Cu_2 by arc-melting; ZrP, ZrS_2, ZrAs, $ZrSe_2$, $ZrTe_3$ by reaction of Z with Zr powder in evacuated silica tubes; $ZrGa_3$, $ZrGe_2$, ZrAg, $ZrIn_2$, $ZrSn_2$, $ZrSb_2$ by similar reactions in tantalum tubes. All of these were examined by powder diffraction for structure types, purities and lattice parameters. The Zr_5Pb_3Z compounds of the volatile P, S, As, and Se were prepared by allowing them to react with stoichiometric amounts of Zr_5Pb_3 powder in silica tubes at 500–600 °C. The products were ground, pelleted, and then sintered in Ta tubes at 1300–1350 °C. The ductility of the container at the end assured the absence of significant nonmetal loss.

A zinc flux was used to grow Zr_5Pb_3Zn crystals starting with preformed Zr_5Pb_3 powder and a 10 fold excess of Zn (Zr:Zn = 1:2) in an alumina crucible which was, in turn, enclosed in an evacuated silica tube. Unreacted zinc slowly evaporated during 7 days at 1000 °C and condensed in a cold region. The residue was pure Zr_5Pb_3Zn as both a black powdery form and a few small rod-like crystals.

Crystals of what were crystallographically identified as Zr_5Pb_{4-x}, X = 0.13 and 0.06, were grown under vapor phase transport conditions with CdI_2 and $ZrCl_4$, respectively, in long (approximately 7 cm) Ta tubes. The first resulted from temperature gradient of 950°/900 °C (external to the jacket) with lead-deficient starting materials at the hot end and 23 days of reaction. Rod-like crystals were found in the cooler end. The second batch (with $ZrCl_4$) were obtained with a 1000°/950 °C gradient with the starting materials at the hot end. In this case, the product crystals were found in the hot end after 7 days of reaction, apparently from more of a mineralization reaction, together with a microcrystalline mixture of Zr_5Pb_3 and Zr_5Pb_4.

Vapor phase transport with $ZrCl_4$ for Z = Al and Zn yielded very large rod crystals up to 3 mm long, but all of these examined crystallographically turned out to be twinned or multiple.

TABLE 1. Selected data collection and refinement information for Zr_5Pb_3Z

Z	Zn	$Pb_{0.87}$	$Pb_{0.94}$
Space group, Z		$P6_3/mcm$; 2	
a[a] (Å)	8.7341 (7)	8.828 (3)	8.851 (1)
c (Å)	5.929 (1)	5.991 (2)	6.009 (1)
$2\theta_{max}$ (°)	45	55	65
Abs. coeff., (cm^{-1}) (Mo K_α)	745	866	880
R, R_w[b]	0.028, 0.032	0.016, 0.024	0.037, 0.041
No. indep. ref.	135	176	278
No. parameters	14	17	17
Sec. ext. coeff. (10^{-7})	–	4.05 (7)	2.92 (5)

[a]From Guinier powder data.
[b]$R = \Sigma ||F_o| - |F_c|| / \Sigma |F_o|$; $R_w = [\Sigma w(|F_o| - |F_c|)^2 / \Sigma w(F_o)^2]^{1/2}$; $w = [\sigma(F)]^{-2}$.

TABLE 2. Reactions in the Zr–Pb binary system

Reactants	Method[a]	Temp. (°C)	Time (d)	Results[b]
Zr, 10Pb	Pb flux	800	7	Zr_5Pb_3 (60), Zr_5Pb_4 (40)
Zr, 10Pb	Pb flux	700	7	Zr_5Pb_3 (5), Zr_5Pb_4 (95)
5Zr, 4Pb	S	800–1000	3	Zr_5Pb_4
1.25Zr, 0.75Zr_5Pb_4	S	1000	7	Zr_5Pb_3
0.625Zr, 0.875Zr_5Pb_4	S	1000	7	Zr_5Pb_3 (50), $Zr_5Pb_{3.65}$ (50)
Zr_5Pb_4 (CdI_2)	V	950/900 0	23	$Zr_5Pb_{3.87}$ crystals
Zr_5Pb_4 ($ZrCl_4$)	V	1000/950 50	7	$Zr_5Pb_{3.94}$ crystals
Zr, 2Pb		500	10	Zr_5Pb_4, Pb
2.75Zr, 0.25Zr_5Pb_4	S	1000	14	A15, Zr + Zr_5Pb_3 (<10 total)
3.75Zr, 0.25Zr_5Pb_4	S	1000	14	A15, Zr + Zr_5Pb_3 (<10 total)
4.75Zr, 0.25Zr_5Pb_4	S	1000	14	A15, Zr (<10)
$Zr_{5.5}Pb$	AM, AN	1000	7	A15 ($Zr_{5.89}Pb$), Zr (~10)
$Zr_{6.5}Pb$	AM, AN	1000	7	A15 ($Zr_{5.71}Pb$), Zr (~10)

[a]S: reactive sintering; V: vapor phase transport; AM: arc-melting; AN: annealing.
[b]Estimated yields based on the powder pattern intensities are given in parentheses (%).

2.3. X-ray studies

Products were routinely examined by Guinier powder diffraction technique with NBS silicon as an internal standard. The lattice parameters of each phase were calculated on the basis of indexed 2θ values measured in the powder patterns.

Single crystals of Zr_5Pb_3Z were sealed in capillaries and data collected for each on a CAD 4 four-circle diffractometer at room temperature for the hexagonal ($P6_3/mcm$) cell. The rather routine refinements were carried out as before [5, 10] and primarily to establish the amount of Z present and the metric details of each structure. Absorption corrections were made with the aid of ψ-scans. Some pertinent data are in Table 1. Tables of structure factor data are available from J.D.C.

2.4. EDX/SEM studies

A JEOL-840 scanning electron microscope was utilized to analyze the compositions of some arc-melted samples of $Zr_{4-6}Pb$ and some single crystals. Samples were polished with a series of sandpapers, ash and then a smooth cloth.

3. Results and discussion

The significant reactions run in the binary Zr–Pb system are summarized in Table 2.

3.1. $Zr_{5-6}Pb$ phase

This compound has been reported to have the cubic Cr_3Si (A15) structure with a tentatively assigned composition of Zr_5Pb [3]. Samples of Zr_xPb, $x=4$, 5, 6, from identical 1000 °C/10 day sintering conditions contained a major amount of the A15 phase with an effectively invariant lattice parameter, $a=5.6619(4)$ Å. Other phases were α-Zr and Zr_5Pb_3 for $x=4$, 5 and only α-Zr for $x=6$, with less than 10% total other phases in each case. The presence of two minor phases in the former pair of samples probably originated with the effect of impurity oxygen, as recently established for the analogous Zr_4Sn system [14]. Impurity oxygen dissolves only in α-Zr, which requires the coformation of Zr_5Pb_3 in stoichiometric or lead-rich systems. Judging from these results, the compound is substantially a line phase, and its composition lies between Zr_5Pb and Zr_6Pb.

The composition was further defined by SEM studies. Separate nominal Zr_6Pb and Zr_5Pb samples were prepared by arc-melting followed by annealing in Ta at 1000 °C for 7 days. Powder patterns showed the A15 phase with the same lattice parameters as above, no Zr_5Pb_3, and about twice as much α-Zr as after the sintering reactions, suggesting heavier contamination by oxygen together with some lead loss in the first step. (It is understandable that the phase was not found in an earlier study in which the metal employed contained approximately 2.6 w/o O [1]). EDX/SEM examination of the samples gave $Zr_{5.89}Pb$ and $Zr_{5.71}Pb$ compositions (± 0.1), respectively, for the major phases. These are reasonably close to each other and, therefore, the composition of the phase is concluded to be near the average, 14.7 at.% Pb or $Zr_{5.80}Pb$. Unlike the analogous Zr_4Sn compound, [5, 14] there was no sign of a superstructure for the lead phase.

3.2. Zr_5Pb_3–Zr_5Pb_4 region

Assessment of the synthetic schemes and results for interstitial compounds of Zr_5Pb_3 requires prior knowledge of its Mn_5Si_3-type structure. Figure 1 shows the hexagonal structure projected along and perpendicular to $\vec{c}$. Two zirconium chains run in the c direction, those built of confacial trigonal antiprisms of Zr2 (Mn2) along 0, 0, z and linear chains of Zr1 (Mn1) at 1/3, 2/3, z, etc., with $z = 0$, 1/2. These metal chains are surrounded by a single type of Pb (Si) atoms that: (i) bridge edges of the shared faces of the trigonal antiprisms of Zr2; (ii) are exo to Zr2 in neighboring chains; (iii) form distorted confacial trigonal antiprisms about Zr1 in the linear chains. The centers of the $(Zr2)_6$ antiprisms in the confacial chains are vacant in the binary structure,

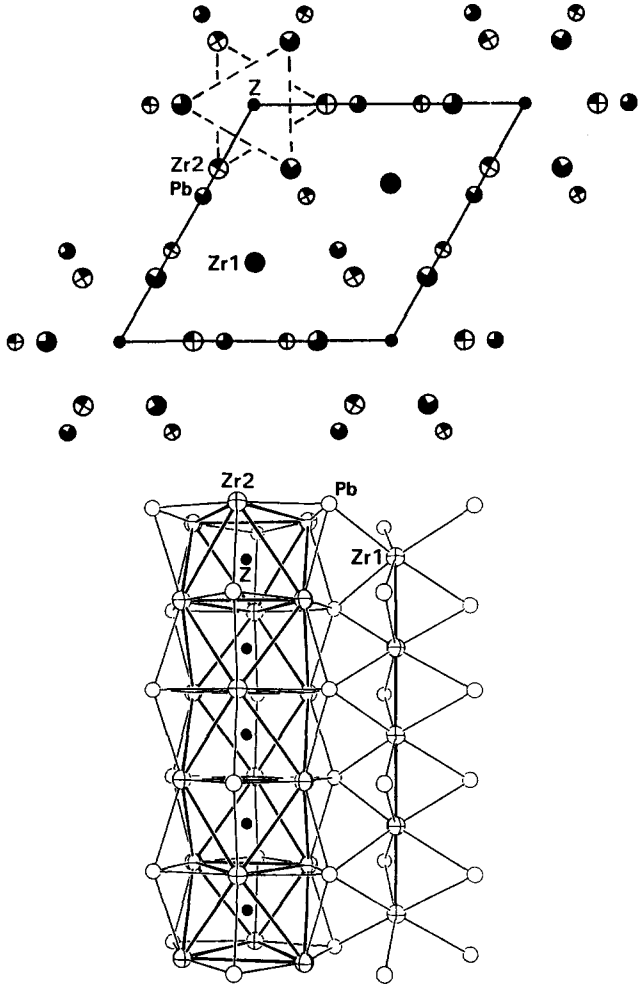

Fig. 1. The stuffed Mn_5Si_3-type (or Ti_5Ga_4) structure of Zr_5Pb_3Z. Top: [001] projection with large circles for Zr, medium circles for Pb, small circles for interstitial Z. The atoms are shaded according to their height in z; solid ones are at $z = 0$, 1/2. One confacial chain of Zr2 atoms is outlined. Bottom: a partial [110] section showing a confacial triangular antiprismatic chain of Zr2 edge-bridged by Pb (left), the linear chain of Zr1 atoms (right) and the shared Pb. (Zr is large, crossed circles, Pb medium and open, and Z, small and solid.)

but these can in many cases be stuffed with diverse interstitial elements (Z) to form Zr_5Pb_3Z compounds with small parametric changes but no other significant alterations in the structure.

Only the Mn_5Si_3-type phase was reported by Nowotny and Schachner [1]. The first evidence for the self-interstitial version of this, Zr_5Pb_4 (Ti_5Ga_4-type [15]), was obtained when zirconium powder was fluxed with 10 fold excess of lead in an alumina crucible at 800 °C for 7 days. The excess lead evaporated during the reaction and condensed at a cooler portion of the jacket. The powder pattern of the black residue contained two hexagonal phases with almost the same line intensities. One of these was later confirmed to be stoichiometric Zr_5Pb_3 based on the lattice parameters while the other had a significantly larger cell. By analogy with Zr_5Sn_4 [5], this was tentatively assigned as Zr_5Pb_4 with lead in the interstitial site. Similar reactions at 700 °C gave about 95% Zr_5Pb_4, the rest Zr_5Pb_3. The Zr_5Pb_4 phase could be repeatedly synthesized in quantitative amounts from the elements via 800–1000 °C reactions at the 5:4 stoichiometry in closed tantalum tubes ($a = 8.873$ (1), $c = 6.019$ (1) Å). Its pattern can also be distinguished from that for Zr_5Pb_3 by the presence of the (001) line only for the latter.

Single crystals of Zr_5Pb_{4-x} were obtained by two vapor phase transport methods (Experimental Section) at or above 900 °C where a phase breadth allows a lead deficiency. That from the CdI_2 vapor transport refined with 86.8 (3) % occupancy for the interstitial lead (Table 3). Since cadmium also forms an interstitial phase Zr_5Pb_3Cd (below), this apparent lead deficiency could also be understood as a fully occupied mixed Cd–Pb site with both Pb and Cd, the latter being approximately 32%. However, an EDX/SEM study of the single crystal showed no cadmium (less than about 0.5%), indicating that the structure refinement likely pertains to the binary system. The smaller lattice parameters ($a = 8.823$ (3), $c = 5.991$ (2) Å) can therefore be justified only with a lead deficiency. The corresponding lead occupancy was 94.0 (5)% for the $ZrCl_4$ transport product, closer to unity but still statistically deficient, and the lattice parameters ($a = 8.851$ (1), $c = 6.009$ (1) Å) are also smaller than for the 5:4 composition.

Sintering Zr and Zr_5Pb_4 at 1000 °C for a Zr_5Pb_3 composition gave a single phase with lattice parameters ($a = 8.5352$ (6), $c = 5.8405$ (7) Å) identical to those tentatively assigned to Zr_5Pb_3 phase from the fluxed reaction. These values differ from the literature value ($a = 8.512$, $c = 5.852$ Å) by 0.01–0.02 Å, but these variances are difficult to interpret because of the sizable amounts of impurities present in the metal used before (Fe, Si, N, C, O) [1]. Sintering a $Zr_5Pb_{3.5}$ composition at 1000 °C gave Zr_5Pb_3 and, for the larger Mn_5Si_3-type

TABLE 3. Refinement parameters for Zr_5Pb_3Z[a]

Atom	Zr_5Pb_3Zn			$Zr_5Pb_{3.868\ (3)}$			$Zr_5Pb_{3.940(5)}$		
	x[a]	occ.	B_{iso}	x	occ.	B_{iso}	x	occ.	B_{iso}
Pb1	0.6157(1)	1	0.40(2)	0.61551(6)	0.996(2)	0.28(1)	0.6154(1)	1.005(3)	0.36(2)
Zr1	1/3	1	0.48(6)	1/3	1	0.26(2)	1/3	1.031(9)	0.42(3)
Zr2	0.2681(3)	1	0.56(5)	0.2799(2)	0.993(4)	0.53(3)	0.2810(3)	1	0.52(4)
Z	0	1.09(6)	0.45(2)	0	0.868(3)	0.25(2)	0	0.940(5)	0.27(2)

[a]Only the Z = Pb composition variables are significant and used for composition calculations.
[b]Atomic positions: Pb1: x, 0, 1/4; Zr1: 1/3, 2/3, 0; Zr2: x, 0, 1/4; Z: 0, 0, 0.

phase, distinctively smaller lattice parameters ($a = 8.7419$ (6), $c = 5.9675$ (6) Å) than for Zr_5Pb_4. The unit cell volumes for the sintered, stoichiometric Zr_5Pb_4 and for the two single crystals that had lead deficiencies exhibit a linear relationship with interstitial Pb content and indicate a limit of about $Zr_5Pb_{3.65}$ in the two-phase system at 1000 °C. Analogy with the Zr_5Sn_3–Zr_5Sn_4 relationship [5] suggests an increased solid solution between Zr_5Pb_3 and Zr_5Pb_4 will occur at higher temperatures. The zirconium-richer component remains a line phase at approximately 1000 °C, whereas Zr_5Pb_4 develops some phase breadth on the lead-poor side above about 800 °C. The relationship at higher temperatures were not explored further.

No phases richer in lead than Zr_5Pb_4 could be found.

3.3. Zr_5Pb_3Z interstitial phases

As summarized in Table 4, most of the phases were synthesized without problems via sintering reactions. The Guinier powder pattern of each product showed a well-defined hexagonal lattice and, with one exception (Te), was free from the lines of any impurity phase, an essential criterion for the formation of a phase with the loaded composition. As will be supported in the next section, the lattice parameters are very sensitive to the interstitials, both type and occupancy, and constant values for both from repeat experiments are also required to conclude a new phase is the stoichiometric interstitial product. Only rarely can relative line intensities offer much help. Lattice parameters of these ternary phases are listed in Table 5.

Some of the phases for which the syntheses required techniques other than simple sintering will be elaborated. Volatile Z elements sometimes give problems in stoichiometric sintering reactions, as others have noted for Zr_5Pb_3 itself [9]. Typical diagnoses of such problems are: (i) lead that was probably gaseous during the reaction is found after the reaction is cooled; (ii) diffuse lines in the powder pattern imply ranges of interstitial content in systems that are not in equilibria, and (iii) lines for additional phases occur in the product's powder pattern. The first problem might be related to the third because in most cases the impurities were ZrZ_x phases. Since P, S, As, and Se, are volatile and corrosive to the Ta containers, these were first reacted with stoichiometric amounts of Zr_5Pb_3 powder in silica tubes at 500–600 °C, and the resulting powders (mixtures) then sintered at 1000 °C in Ta. The products so obtained did not show any of the problems listed above.

The synthesis of the cadmium interstitial phase presented the same problem, and its accomplishment is noteworthy since the analogue was not achieved with Zr_5Sn_3 or Zr_5Sb_3. The synthesis was first attempted with a stoichiometric amount of Cd vapor and Zr_5Pb_3 powder. However, the reaction was not complete after 11 days at 1000 °C; about half of the Zr_5Pb_3 had an expanded lattice ($a = 8.790$ (2) and $c = 5.966$ (2) Å), and Cd drops were condensed on an apparent cold spot from a temperature gradient in the furnace. The lattice parameters could not be taken for those of the stoichiometric phase under these circumstances. However, many whisker crystals formed on top of what had been Cd(ℓ) when a similar reaction was performed at 700 °C with Cd:Zr = 1:1. No other phase was present, and the lattice parameters of the whiskers, $a = 8.8240$ (6), $c = 5.9876$ (7) Å, fit the trend of cell volumes and c/a for phases with Z = Ag–Sn very well (below). Unfortunately, these crystals grew as multiples with common a–b planes according to Weissenberg film studies, and their structural study was not possible.

As already shown for Zr_5Pb_3–Zr_5Pb_4, Zr_5Sn_3–Zr_5Sn_4 [5], Zr_5Sb_{3+x} [16], and $Zr_5Sn_3S_x$ [11], some interstitial phases of this type can be substoichiometric, often at higher temperatures. Although others were not investigated extensively in this work, copper also appears to show some substoichiometry but with a rather small range. The stoichiometrically loaded Zr_5Pb_3Cu repeatedly gave $a = 8.6847$ (6) and $c = 5.9123$ (7) Å while a $Zr_5Pb_3Cu_{1/2}$ product was composed of Zr_5Pb_3 and $Zr_5Pb_3Cu_x$, the latter with $a = 8.671$ (1), $c = 5.913$ (1) Å. Notice that the c-parameter is now constant, in contrast to $Zr_5Sn_3S_x$. The literature values for the lattice dimensions of Zr_5Pb_3Cu prepared in SiO_2, $a = 8.665$, $c = 5.926$ [13], are contradictory in that they deviate by

TABLE 4. Syntheses of Zr_5Pb_3Z interstitial phases

Z	Reactants[a]	Method[b,c]	T (°C), d	Remarks[d]
Al	$ZrAl_2$	V	1000/900, 20	Twinned crystals
		S	1000, 11	
Si	Si	S	1000, 16	
P	Zr_5Pb_3, P	R[e]	500, 7	
		S	1000, 11	
S	Zr_5Pb_3, S	R[e]	500, 7	
		S	1100, 13	
Fe	$ZrFe_2$	S	1350, 3	
Co	$ZrCo_2$	S	1350, 3	
Ni	$ZrNi_2$	S	1350, 3	
Cu	Zr_3Cu_2	S	1000, 8	
Zn	Zr_5Pb_3, Zn (xs)	F	1000, 7	Single crystals
	$ZrZn_2$ ($ZrCl_4$)	V	1000/950, 20	Twinned crystals
Ga	$ZrGa_3$	S	1000, 7	
Ge	$ZrGe_2$	S	1350, 3	
As	Zr_5Pb_3, As	R[e]	500, 7	
		S	1000, 11	
Se	Zr_5Pb_3, Se	R[e]	500, 7	
		S	1000, 9	
Ag	ZrAg	S	1000, 13	
Cd	Zr_5Pb_3, Cd (xs)	F	700, 7	Whiskers of multiple crystals
In	$ZrIn_2$	S	1000, 11	
Sn	$ZrSn_2$	S	1000, 11	
Sb	$ZrSb_2$	S	1350, 5	
Te	$ZrTe_3$	S	1000, 16	Zr_3Te_2 impurity (<10%)

[a]The Z element sources are listed. Zr and Zr_5Pb_4 powders were also employed unless otherwise specified.
[b]Ta containers unless noted.
[c]V: vapor phase transport; S: sintering; R: direct reaction of Zr_5Pb_3 and element Z in SiO_2 container; F: fluxed reaction.
[d]Single phase products were obtained unless otherwise noted.
[e]These reactions were performed in the sequence R, S.

0.01–0.02 Å from ours, but in opposite directions, the same as found for Zr_5Pb_3 (above). Impurities complicate the ternary comparison as well.

Syntheses of some interstitial compounds were tried via vapor phase transport reactions. Crystal growth was obtained with $ZrCl_4$ but not ZrI_4 even through thermodynamic estimates suggested the latter would be better. Needle crystals up to 3 mm long were obtained for Zr_5Pb_3Al and Zr_5Pb_3Zn phases as well as for Zr_5Pb_{4-x}, with almost complete material transport for the first two starting with stoichiometric mixtures of Zr_5Pb_4, Zr and ZrZ_x powders. However, the first two crystals showed apparent twinning problems so that crystal structure refinements could not be pursued. Premade compounds with Z = P, S, As, Se, Cu, Ge, Cd, or Ag that were equilibrated with $ZrCl_4$ gave no apparent recrystallization or only other products like Zr_3S_2.

Unsuccessful synthesis reactions were obtained with early transition elements like Cr and Mn. Sintering at 1350 °C apparently causes loss of these Z elements, probably as a solid solution in Ta for Cr. The lattice parameters obtained were identical to those for the empty Zr_5Pb_3, and an EDX/SEM study on the Cr sample showed no incorporation.

Sintering of the manganese or iron systems at 1000 °C for 19 d instead gave two distinctly different Mn_5Si_3-type products, one distinctly too large to be considered a Zr_5Pb_3Z product and the other, even smaller than the host. These parallel observations made for the Zr_5Sn_3Fe systems [11]. Here as well, the two products probably represent a Zr_5Pb_3(Pb,Z) mixed phase with substantial lead content and a substitution product with or without interstitial. On the other hand, sintering of the appropriate components to produce Zr_5Pb_3Z, Z = Fe, Co, Ni, at 1350 °C gave reasonably-sized, one-phase products by X-rays. A magnetic study of the iron product did show a very weak signal that was very similar to the result for the strongly ferromagnetic $ZrFe_2$, the presence of which would probably be countered by correspondingly small amount of a mixed interstitial $Zr_5Pb_3(Fe_{1-x}Pb_x)$.

These results are in some contrast with those for iron in the Zr_5Sn_3 and Zr_5Sb_3 substrates. The fully stoichiometric ternary was unstable in both systems, even at elevated temperatures. Instead, the precipitation

TABLE 5. Lattice parameters and derived data for Zr_5Pb_3Z (Å)[a]

Z	a	c	V	c/a
Al	8.7871(5)	5.9460(7)	397.60(6)	0.677
Si	8.6830(6)	5.8968(7)	385.03(7)	0.679
P	8.6044(5)	5.9660(8)	382.52(7)	0.693
S	8.5789(7)	6.0027(9)	385.60(8)	0.698
Fe	8.705(1)	5.922(1)	388.6(1)	0.680
Co	8.6832(5)	5.8851(5)	384.28(5)	0.678
Ni	8.6261(7)	5.8916(8)	379.66(8)	0.683
Cu	8.6847(6)	5.9123(7)	386.19(7)	0.681
Zn	8.7341(7)	5.929(1)	391.70(9)	0.679
Ga	8.7451(5)	5.9230(6)	392.29(6)	0.677
Ge	8.6924(6)	5.9128(8)	386.90(7)	0.680
As	8.6298(8)	5.953(1)	383.9(1)	0.690
Se[b]	8.6312(8)	5.9796(9)	385.78(9)	0.693
Ag	8.767(2)	5.965(2)	397.0(2)	0.680
Cd	8.8240(6)	5.9876(7)	403.76(7)	0.679
In	8.8458(7)	5.9989(8)	406.50(9)	0.678
Sn	8.838(1)	6.000(1)	405.9(1)	0.679
Sb	8.664(1)	5.937(1)	386.0(1)	0.685
Te	8.6770(7)	5.964(1)	388.9(1)	0.687
–	8.5352(6)	5.8405(7)	368.48(7)	0.684
Pb	8.873(1)	6.019(1)	410.4(1)	0.678

[a]Stuffed-Mn_5Si_3 (Ti_5Ga_4) type (space group $P6_3/mcm$).
[b]Average for more than one sample.

TABLE 6. Important distances in Zr_5Pb_3Z (Å)

Bond type		Z		
		Zn	$Pb_{0.87}$	$Pb_{0.94}$
Zr2–Z	2x	2.771(6)	2.889(1)	2.912(2)
Zr2–Pb				
Interchain	1x	3.036(7)	2.962(2)	2.967(3)
Out of plane	2x	3.133(2)	3.135(4)	3.1469(8)
In plane	2x	2.982(2)	3.0391(5)	3.0586(9)
Zr1–Pb	6x	3.0944(8)	3.1266(2)	3.1420(3)
Zr2–Zr2				
Out of plane	4x	3.778(4)	3.8830(6)	3.908(1)
In plane	2x	4.06(1)	4.279(2)	4.308(2)
Zr1–Zr2	6x	3.558(4)	3.5370(8)	3.550(1)

of $ZrFe_2$ produced mixed interstitial products $Zr_5M_3(M_xFe_y)$, M = Sn Sb, $1/3 < x, y < 2/3, x+y \leq 1$ [11, 17]. Single phase products were obtained for arc-melted $Zr_5Sn_{3.3}Z_{0.3}$, Z = Fe, Co, Ni, however, and these did not change after 8 days at 1300 °C.

3.4. Crystal chemistry

Even though there are not many single crystal results for the lead family, comparison among these provides a valuable insight into the nature of the interstitial chemistry. Similar studies for Zr_5Sn_3 and Zr_5Sb_3 hosts help with some generalizations regarding interstitial compounds in this structure type.

Table 6 lists important atomic distances for the three Zr_5Pb_3Z single crystal refinements. The biggest effect of the interstitial is again [12] the lateral expansion of the trigonal antiprism in the shared faces. As in other examples, the Zr2–Z interactions appear to be remarkably strong. The Zr2–Zn bond distance in Zr_5Pb_3Zn, 2.771 (6) Å, is only slightly longer than in Zr_5Sb_3Zn, 2.747 (1) Å, probably because of a matrix effect from the larger lead. But these Zr2–Zn separations are distinctly less than in ZrZn (CsCl), 2.89 Å [18], or the more distant $ZrZn_2$ (Cu_2Mg), 3.07 Å [19], where Zn has 6+6 coordination. This is similar with the self interstitial in $Zr_5Pb_{3.94}$; the Zr2–Pb2 (interstitial) distance, 2.912 Å, is notably shorter than the average Zr–Pb1 distances, 3.105 Å. This may reflect in part a difference in coordination number, six for Pb2 (Z) *vs.* nine for Pb1, but distinctly shorter bonds at the interstitial site may be general. Sufficiently well defined examples of other Ti_5Ga_4-type structures appear limited to Nb_5Ga_4, where d(Nb–Ga2) is 2.608 (×6) Å *vs.* 2.794 Å (×9) in the framework; these compare with d(Nb–Ga) values in Nb_5Ga_3 (W_5Si_3-type) of 2.72 Å (×8) about Ga1 centering the antiprisms and 2.73 Å (×6) plus 2.93 Å (×4) about Ga2 [20]. Coordination number does not seem to affect Zr–Si distances in a variety of binary phases significantly, and these are again greater than that in Zr_5Sb_3Si [12].

All of the refined crystal structures showed that the host lattices were essentially complete and stoichiometric. The same observation has been made for several Zr_5Sn_3Z systems [11]. Thus, there is only one variable affecting the lattice parameters listed in Table 5, that is, the nature and amount of Z. The unit cell volumes for Zr_5Pb_{4-x}, 404.3, 407.7 and 410.4 Å^3 for $x = 0.13$, 0.06, and 0, respectively, exemplify the sensitivity of the lattice constants to occupancy. Since the interstitial event is always accompanied by expansion of the host lattice (except for the second period Z in Zr_5Sn_3 [11] and Zr_5Sb_3 [12] hosts), the larger values of lattice parameters when more than one hexagonal phase is observed have always been assumed to correspond to the more nearly stoichiometric one.

The unit cell volumes of the lead interstitial phases are plotted in Fig. 2 according to the periodicity of Z. All of these represent sizable expansions as the empty Zr_5Pb_3 has a cell volume of only 368.5 Å^3, off-scale in the figure. (We expect C, N, O would have *ca.* zero to small negative partial molar volumes on the basis of other results [11, 12], but these systems were not investigated.) Cell volumes increase gradually from the copper to the aluminum or silicon families, but beyond this they decrease sharply. The subsequent leveling off or upturn in volume for pnictide and chalcogenide may result from the repulsion of contiguous Z elements along $\vec{c}$ for those Z that are more negative. This is more evident for the related Zr_5Sb_3Z [12], but repulsion is still present and striking with lead as well when

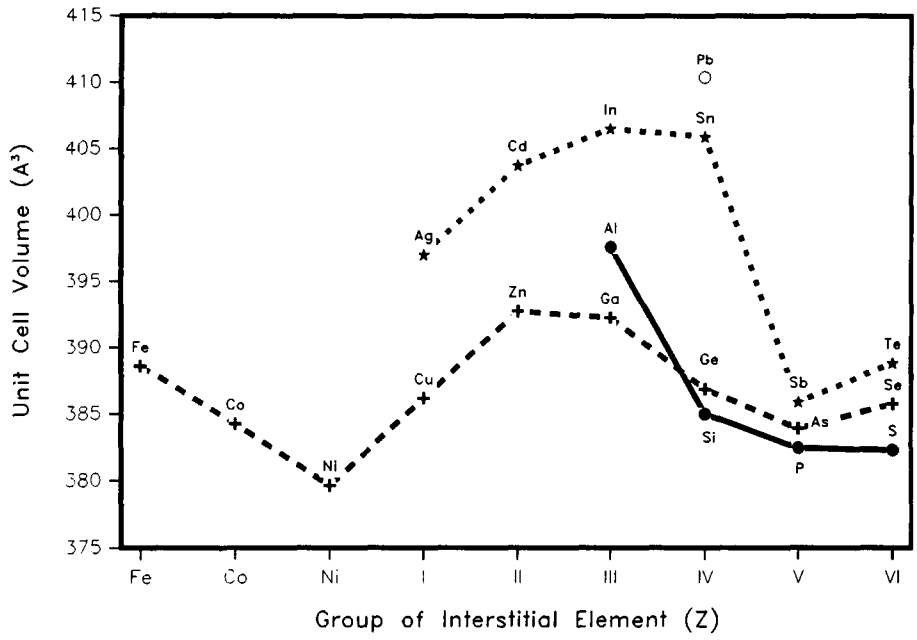

Fig. 2. Unit cell volumes of Zr_5Pb_3Z according to the periodicity of Z. ●, +, ★, and ○ represent 3rd, 4th, 5th and 6th period Z, respectively.

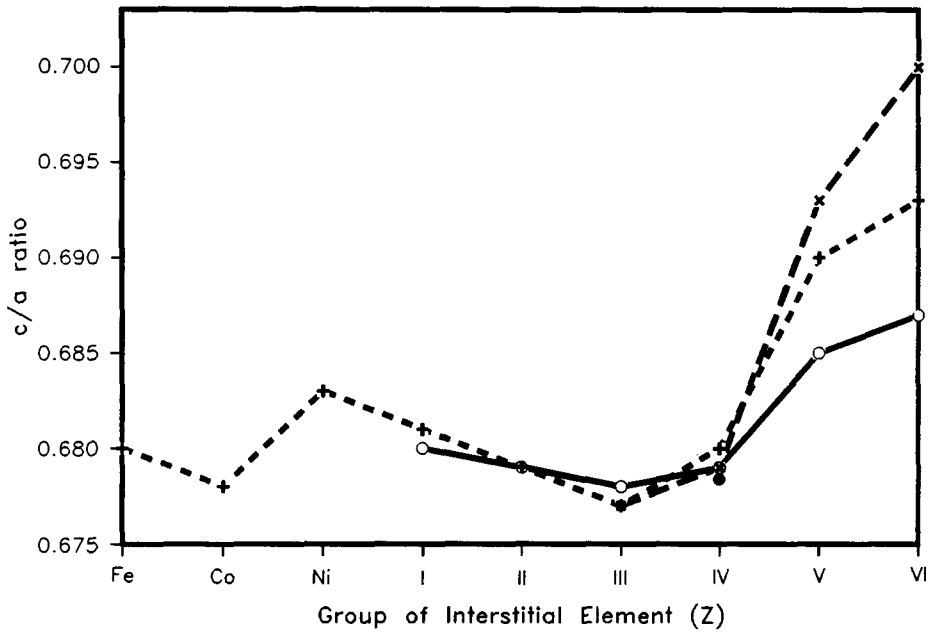

Fig. 3. *c/a* ratios for Zr_5Pb_3Z phases as a function of period and group of Z. ×, +, ○ and ● identify 3rd, 4th, 5th and 6th period Z, respectively. × = Al–S, + = Fe–Se and ○ = Ag–Te.

viewed in terms of the *c/a* ratios, Fig. 3. The chalcogenide–chalcogenide separations in these compounds ($c/2 \simeq 3.0$ Å) are distinctly less than the shortest contact separations observed in many reduced transition metal chalcogenides, approximately 3.3 Å for sulfides and approximately 3.4 Å for selenides [21].

Admittedly, the cell volumes represent a conglomeration of effects, not just the incremental expansion because of Z but also changes of Zr–Pb bond lengths in the sheathing and interbridging functions about the Zr chains. Several structures that have been quantified suggest that the interchain bridging bonds act in some opposition to expansion or contraction produced by Z. Still, the composite effects of Zr–Pb distance changes may be relatively uniform so that volumes still reflect something of effective Z increments. Indeed, the general volume changes for Z in Zr_5Pb_3 (Fig. 2) as well as in Zr_5Sn_3 [11] along the periods follow trends in Pauling's

table of metallic/covalent radii [22] fairly well, and also for the less extensive results for Zr_5Sb_3 [12]. The drop at Zr_5Pb_3Sb is unexpected on this basis, however, while the upturns for the chalcogenides have already been dealt with. Inclusion of a significant number of fifth period (Ag–Te) interstitials in the lead host gives us a new view of the volume effects relative to those for third and fourth period Z. Vertical changes within the groups in Fig. 2 are distinctly nonlinear, with considerable volume similarities between 3rd *vs.* 4th period Z but noticeable expansions for the fifth period members, Ag, Cd, In, Sn, especially. In fact, such a behavior is already exhibited in the same radii data given by Pauling. The considerable size similarity of 4th *vs.* 3rd period elements has been considered in terms of the effects of a "**3d** contraction", while the size increases for the 5th period (except at Sb) are more nearly normal once the effects of the lanthanides have died out. We have no immediate explanation for what seems to be a modestly anomalous volume datum for Zr_5Pb_3Al.

The chemistry represented by such large families of isostructural, interstitial derivatives is unusual since all of these phases are electron-rich and metallic rather than electronically precise. A great many pairs of elements exhibit an Mn_5Si_3-type phase, and it is possible to select among these such that only a few excess electrons remain in the binary, *e.g.* $5 \cdot 3 - 3 \cdot 4 = 3$ in La_5Ge_3. In these cases, it has proven possible to "tune" this count to zero with a suitable interstitial (*e.g.* As) and to produce valence (Zintl) phases [23]. No doubt a great many mixed interstitial products are also possible.

4. Summary

The Zr–Pb binary system shows much similarity to that of Zr–Sn, namely the off-stoichiometric A15 phase and isostructural Zr_5M_3 and Zr_5M_4 phases, with an extensive solid solution between the latter pair at higher temperatures. Like Zr_5Sn_3, Zr_5Pb_3 can accommodate many main-group and several late transition-metal elements. However, the family of Z for the larger Zr_5Pb_3 includes larger elements like Cd, Ag, In, and Te that were not bound in other smaller hosts studied. The crystal structures of the interstitial phases show that the host structures greatly expand to provide room for the larger interstitial elements. The strength of the Zr–Z bonding probably dominates all of these systems.

Acknowledgments

The authors are indebted to H. F. Franzen, K. Gschneidner and L. Daniels for the continued provision of arc-melting, Ta-welding and X-ray diffractometer facilities, and to S. C. Sevov for the SEM examinations. This research was supported by the US Department of Energy, Office of Basic Energy Sciences, Materials Sciences Division. The Ames Laboratory is operated for the Department of Energy by Iowa State University under contract No. W-7405-Eng-82.

References

1 H. Nowotny and H. Schachner, *Monatsh. Chem., 84* (1953) 169.
2 H. Nowotny, H. Auer-Welsbach, J. Bruss and A. Kohl, *Monatsh. Chem., 90* (1959) 15.
3 J. O. Scarborough and J. O. Betterton Jr., *US Atomic Energy Comm. ORNL-3470*, 1963, p. 26.
4 R. Flükiger, in S. Foner and B. B. Schwarz (eds.), *Superconductor Materials Science*, Plenum, New York, 1981.
5 Y.-U. Kwon and J. D. Corbett, *Chem. Mater., 2* (1990) 27.
6 T. B. Massalski (ed.), *Binary Alloy Phase Diagrams,* Vol. 3, ASM, Metals Park, OH, 2nd edn., 1991, p. 3032.
7 M. D. Donne, U. Fischer and M. Küchle, *Nucl. Technol., 71* (1985) 15.
8 M. Song, M. Z. Youssef, M. A. Abdou and A. R. Raffray, *Fusion Eng. Des., 10* (1989) 47.
9 M. D. Donne, S. Dorner and D. F. Lupton, *J. Nucl. Mater., 141* (1986) 369.
10 E. Garcia and J. D. Corbett, *J. Solid State Chem., 74* (1988) 440.
11 Y.-U. Kwon and J. D. Corbett, *Chem. Mater.* 1992, 4, in press.
12 E. Garcia and J. D. Corbett, *Inorg. Chem., 29* (1990) 3274.
13 W. Rieger, H. Nowotny and F. Benesovsky, *Monatsh. Chem., 96* (1965) 232.
14 Y.-U. Kwon and J. D. Corbett, *Chem. Mater., 4* (1992) 187.
15 M. Pötzschke and K. Schubert, *Z. Metallk., 53* (1962) 474.
16 E. Garcia and J. D. Corbett, *Inorg. Chem., 27* (1988) 2353.
17 Y.-U. Kwon, S. C. Sevov and J. D. Corbett, *Inorg. Chem., 2* (1990) 550.
18 N. F. Lashko and G. I. Morozova, *Kristallograf., 14* (1969) 143.
19 S. Ogawa, *J. Phys. Soc. Jpn., 25* (1968) 109.
20 M. Drys, R. Kubiak and K. Lukaszewicz, *Bull. Acad. Pol. Sci., Ser Sci. Chim., 21* (1973) 901, 907.
21 J. D. Corbett, *J. Solid State Chem., 39* (1981) 62.
22 L. Pauling, *The Nature of Chemical Bond*, Cornell University Press, Ithaca, NY, 3rd edn., 1960, pp. 246–247.
23 A. M. Guloy and J. D. Corbett, unpublished work.